biologia plantarum
an international journal for experimental botany

BIOLOGIA PLANTARUM (2024) 68: 139-151 DOI: 10.32615/bp.2024.012

Integrated transcriptomic and metabolomic analyses provide insights into the response of tobacco axillary buds to exogenous strigolactone

Boxi TANG[1,2], Huiyuan TIAN[1,2], Wuwei FAN[3], Zhiyan PAN[1,2], Yuanxiu WANG[1,2], Jiantao PENG[1,2], and Guoqin LIU[1,2,*]

[1] *College of Tobacco Science, Guizhou University, Guiyang 550025, China*
[2] *Key Laboratory of Tobacco Quality Research in Guizhou Province, Guiyang 550025, China*
[3] *Yimen County Branch of Yuxi Tobacco Company, Yimen, Yunnan 651100, China*

[*]Corresponding author: E-mail: liuguoqin75@126.com

Abstract

Strigolactones (SL) are crucial plant hormones that regulate plant growth. We investigated genetic and metabolic changes in tobacco axillary flower buds following application of GR24 (SL synthetic analogue), administered 2 and 6 days later. The results indicated that GR24 effectively inhibited the growth of axillary buds. RNA sequencing revealed 1 781 differentially expressed genes in axillary buds after 6 days of GR24 treatment compared to untreated controls. Among them, 882 genes were up-regulated following GR24 treatment, suggesting substantial number of genes experienced significant changes in expression following GR24 treatment. Four carbohydrate metabolites exhibited altered abundance after 6 days of GR24 treatment; one increased and three decreased. In this study, GR24 induces substantial changes in the transcriptome and metabolome of tobacco axillary buds, with the starch and sucrose metabolic pathways and the phenylpropane biosynthesis pathway playing essential roles in the regulation of tobacco axillary bud development. Transcriptomic and metabolomic analyses highlighted that GR24 treatment significantly modulated the starch and sucrose metabolic pathways and the phenylpropane biosynthesis pathway. Our results suggest that the metabolic pathways of starch and sucrose and the biosynthesis pathway of phenylpropane play important roles in the regulation of growth and development of tobacco axillary buds by GR24.

Keywords: axillary buds, exogenous strigolactone treatment, omics integration, tobacco.

Introduction

Plant axillary bud growth is closely related to sugar metabolism. Studies have shown that the generation of apical dominance is the result of the competition between apical buds and axillary buds for limiting carbon sources (Mason et al., 2014). Saccharide plays a significant role in regulating the dormancy and growth of plant axillary buds (Barbier et al., 2015a; Patil et al., 2022). After decapitation, the sucrose concentration in the axillary buds increases significantly. Treatment with exogenous sucrose solution can significantly promote the growth of axillary buds (Satoh-Nagasawa et al., 2006), therefore, the study of sugar metabolism in axillary buds is of great importance. In addition to the effect of sugar metabolism, plant axillary bud growth is also regulated by a variety of factors such as genetic factors, light, and plant hormones (Horvath et al., 2002; Liu, 2012; Barbier et al., 2021). Plant

Received 29 April 2024, *last revision* 1 July 2024, *accepted* 7 August 2024.
Abbreviations: BP - biological process; CC - cellular component; CK - cytokinin; DEGs - differentially expressed genes; DEMs - differentially expressed metabolites; FDR - false discovery rate; GA - gibberellin; *GO* - gene ontology; GR24 - SL synthetic analogue; IAA - auxin; *KEGG* - the Kyoto Encyclopedia of Genes and Genomes; MEs - module eigengenes; MF - molecular function; PCA - principal component analysis; QC - quality control; SL - strigolactone; SPS - sucrose-phosphate synthase; SuSy - sucrose synthetase; T6P - trehalose 6-phosphate phosphatase; UPLC - ultra performance liquid chromatography; WGCNA - weighted gene co-expression network analysis.
Acknowledgements: This research is funded by the National Natural Science Foundation of China (Grant No. 32060420).
Conflict of interest: The authors declare that they have no conflict of interest.

hormones, such as auxins (IAA), cytokinins (CK), and gibberellins (GA), have been studied for their influence on axillary bud growth and development; and in recent years, the regulation of axillary bud growth by plant hormones has become a hot topic for research. IAA is used in plant growth regulation studies and can affect the outgrowth of axillary buds (Balla et al., 2016). CK can promote the development and growth of axillary buds by increasing cell division, differentiation, and growth of various tissues and show synergistic effects with plant auxins (Waldie and Leyser, 2018; Qiu et al., 2019). GA play a vital role in the overall growth of crops and promote the growth of axillary buds in many plants (Ni et al., 2017). Additionally, in recent years, it has been found that strigolactones (SL) have a negative regulatory effect on the growth and development of plant axillary buds (Kaniganti et al., 2022).

SL are a recently discovered group of carotenoid-derived phytohormones (Zwanenburg and Blanco-Ania, 2018) that have been found to play an inhibitory role in the control of axillary bud outgrowth and development in apples, peas, and *Arabidopsis thaliana* (Brewer et al., 2009; Tan et al., 2019; Wang et al., 2020a). GR24 is a synthetic analog of SL and has been widely used in the study of the growth and development of plant axillary buds. Exogenous application of GR24 reduces the formation of *Cephaelis ipecacuanha* axillary buds (Okazaki et al., 2021). Low amounts of GR24 were found in some mutants with an increased axillary bud phenotype and application of GR24 inhibited the branching of these mutants (Guan et al., 2012; Kotov and Kotova, 2018). Various studies have shown that sucrose, GR24, and IAA have an antagonistic role in the control of axillary bud growth. Sucrose can hinder SL signal transduction and axillary bud growth (Finlayson, 2022). IAA and sugar availability predominantly influences SL signaling, which is induced by auxin to inhibit bud growth. Nevertheless, sugar availability can offset this inhibitory action (Bertheloot et al., 2020).

An increasing number of studies have shown that plant secondary metabolites, such as terpenes, phenols, and various nitrogen-containing compounds, play vital roles in regulating plant growth and development (Wang et al., 2020b; Shi et al., 2021). Phenylpropanoid metabolism is an important secondary metabolic pathway that dominates the synthesis of these secondary metabolites. In recent years, a large number of studies have revealed the enzymatic processes involved in plant phenylalanine metabolism and the regulatory mechanism of the entire phenylalanine metabolic pathway. This has provided a preliminary understanding of this pathway and a theoretical basis for the genetic improvement and artificially directed synthesis of specific secondary metabolites in plants (Dong and Lin, 2021). However, the metabolism of phenylpropane has not been studied in detail in all plants and the research in tobacco axillary buds is still lacking.

In tobacco, the quality of leaf harvest is an important economic indicator. Plant axillary buds have an important impact on the yield and quality of tobacco leaves, thereby affecting economic benefits (Pal and Kadam, 1949). Previous studies have shown that SL can inhibit the growth of axillary buds and most of the studies have focused on the phenotype, physiology, biochemistry, and molecular mechanisms of axillary buds (Gomez-Roldan et al., 2008). However, there are few studies focusing on effects of SL on the key metabolic pathways that regulate axillary bud growth in tobacco.

In this study, the tobacco cultivar Yunyan 87 was used as the experimental material. We performed a combination of morphological observations and transcriptomic and metabolomic analyses to investigate the effect of SL on the growth and key metabolic pathways of tobacco axillary buds. The findings reported in this study will improve our understanding of the molecular mechanisms underlying SL inhibition of axillary bud outgrowth.

Materials and methods

Plant material and hormone processing: The tobacco (*Nicotiana tabacum* L.) cultivar Yunyan 87 used in this study was provided by the *Meitan County Branch* of the *Guizhou Tobacco Company*. Carefully selected tobacco seeds were sown in 12-hole nursery boxes (72 mm long, 49 mm wide, 62 mm high) with 0.85 L of water per box and 1 seedling per hole. When the seedlings had five leaves, those with uniform growth were selected and transplanted to individual plastic pots (32 cm diameter, 19.5 cm height). Each pot contained 10 kg of soil and the ratio of soil to tobacco seedling substrate was 6:1. The 120 potted plants were divided into two groups: the control (C) and the GR24 treatment group, with 60 plants in each group. Each group was further subdivided into two treatment durations: 2 d and 6 d. Three replicates were performed for each treatment duration, with 10 plants per replicate. The plants were cultivated outdoors, watered regularly, and evenly capped at the budding stage. After topping, 100 µL of GR24 solution (10 µmol/L) was applied to the leaf axils at the first to third nodes at the top of the plants in the GR24 group, while the C group was not treated after topping, plants were treated daily. After topping, axillary buds were collected with a sterile razor blade and immediately placed in a ziplock bag. The samples were then snap-frozen in liquid nitrogen before storing in a freezer at –80°C for metabolomic and transcriptomic experiments.

Morphological index measurement: The node where the first leaf after topping was located was taken as the starting node for the measurement of axillary buds and the length of the axillary buds of the three nodes in turn was recorded. The lengths of the axillary buds of nodes 1 - 3 were measured with a ruler on days 2 and 6 of the treatment.

RNA extraction, library construction, and sequencing: The extraction of axillary buds RNA of the mixed nodes 1 - 3 was done at days 2 and 6 of the treatment. Total RNA was extracted using the *TRIzol* reagent kit (*Thermo Fisher Scientific*, Waltham, MA, USA), according to the manufacturer's protocol. RNA quality was assessed using an *Agilent 2100 Bioanalyzer* (*Agilent Technologies*,

Santa Clara, CA, USA) and RNase-free agarose gel electrophoresis. After total RNA was extracted, eukaryotic mRNA was enriched using oligo(dT) beads, whereas prokaryotic mRNA was enriched by removing rRNA using a *Ribo-Zero*™ magnetic kit (*Epicenter*, Madison, WI, USA). The enriched mRNA was then fragmented into short fragments using fragmentation buffer and reverse transcribed into cDNA using random primers. Second-strand cDNA was synthesized using DNA polymerase I, RNase H, dNTPs, and buffer. The cDNA fragments were then purified with a *QIAquick* PCR extraction kit (*Qiagen*, Venlo, The Netherlands), end-repaired, A base added, and ligated to *Illumina* sequencing adapters. The ligation products were size-selected by agarose gel electrophoresis, PCR-amplified, and sequenced using an *Illumina Hiseq 2500* by *Gene Denovo Biotechnology Co.* (Guangzhou, China).

Reads obtained from the sequencing machines include raw reads containing adapters or low-quality bases which will affect the following assembly and analysis. Thus, to get high-quality clean reads, reads were further filtered by *fastp version 0.18.0* (Chen et al., 2018). The parameters were as follows: removing reads containing adapters; removing reads containing more than 10% of unknown nucleotides (N); removing low-quality reads containing more than 50% of low-quality (Q-value ≤ 20) bases. The rRNA mapped reads then will be removed. The remaining clean reads were further used in assembly and gene abundance calculation. Short reads alignment tool *Bowtie2 version 2.2.8* (Langmead and Salzberg, 2012) was used for mapping reads to ribosome RNA (rRNA) database. An index of the reference genome was built, and paired-end clean reads were mapped to the reference genome using *HISAT2 2.1.0* (Kim et al., 2015) and other parameters set as a default. The mapped reads of each sample were assembled by using *StringTie version 1.3.1* (Pertea et al., 2015; 2016) in a reference-based approach. For each transcription region, a FPKM (fragment per kilobase of transcript per million mapped reads) value was calculated to quantify its expression abundance and variations, using *RSEM* (Li and Dewey, 2011) software. The FPKM formula is shown as follows:

$$F = \frac{10^6 C}{NL/10^3}$$

where F is FPKM, given FPKM(i) is the expression of gene i, C is number of fragments mapped to gene i, N is total number of fragments that mapped to reference genes, and L is number of bases on gene i. The resulted sequence data were submitted to National Center for Biotechnology Information, U.S. National Library of Medicine (*NCBI*;· https://www.ncbi.nlm.nih.gov/geo/query/acc.cgi?acc=GSE233880) under the accession number GSE233880.

Differentially expressed genes (DEGs): Differential expression analysis of the RNA-Seq data was performed using *DESeq2* software (Love et al., 2014) between two different groups and by *edgeR* (Robinson et al., 2010) between two samples. Genes or transcripts with a false discovery rate (FDR) below 0.05 and absolute fold change ≥ 2 were considered differentially expressed.

Gene ontology (*GO*) enrichment analysis: All DEGs were mapped to *GO* terms in the gene ontology database (http://www.geneontology.org/), gene numbers were calculated for every term, and significantly enriched *GO* terms in DEGs compared to the genome background were defined by a hypergeometric test. The calculating formula for the *P*-value was:

$$P = 1 - \sum_{i=0}^{m-1} \frac{\binom{M}{i}\binom{N-M}{n-i}}{\binom{N}{n}}$$

where N is the number of all genes with *GO* annotation, n is the number of DEGs in N, M is the number of all genes that are annotated to certain *GO* terms, and m is the number of DEGs in M. An FDR correction was applied to the calculated *P*-values and an FDR-adjusted *P*-value ≤ 0.05 was considered significant. *GO* terms meeting this condition were defined as significantly enriched within the DEGs. This analysis was able to determine the main biological functions of the DEGs.

Pathway enrichment analysis: Biological functions are usually performed by interactions between groups of genes. Pathway-related database analysis helps to further understand the biological functions of genes. The Kyoto Encyclopedia of Genes and Genomes (*KEGG*) is a major public pathway-related database and can be used in pathway enrichment analysis identified significantly enriched metabolic pathways or signal transduction pathways in DEGs compared to the whole-genome background. The calculation formula was the same as that used in the *GO* analysis:

$$P = 1 - \sum_{i=0}^{m-1} \frac{\binom{M}{i}\binom{N-M}{n-i}}{\binom{N}{n}}$$

where N is the number of all genes with *KEGG* annotation, n is the number of DEGs in N, M is the number of all genes annotated to specific pathways, and m is the number of DEGs in M. An FDR correction was applied to the calculated *P*-values and an FDR-adjusted *P*-value ≤ 0.05 was considered significant. Pathways meeting this condition were defined as significantly enriched pathways within the DEGs.

Weighted gene co-expression network analysis (WGCNA) and visualization of gene networks: The *WGCNA R* package was used to construct a weighted gene co-expression network (Langfelder and Horvath, 2008), selecting only genes with expressions ≥ 5 to construct the network. A total of 20 056 genes were used for WGCNA. After removing outliers, Pearson correlations between all paired genes were constructed according to the correlation matrix. Using the dynamic tree cutting method to identify the modules, 17 modules

were identified by consensus. The characteristic genes for each module, module eigengenes (MEs), were calculated and were defined as the first principal component of the module, representing the overall expression level of the module. Cluster analysis was performed based on the average distance between modules, which was determined by Pearson correlation analysis between MEs separating the modules. Those modules with high similarity were then merged, with a merge threshold function of 0.25.

Metabolite extraction and detection: The extraction of axillary buds metabolite was done in the mix from 1 - 3 nodes at days 2 and 6 of the treatment. The axillary bud samples were removed from storage and lyophilized (*Thermo Scientific Forma 900 Series*). The samples were then ground for 1.5 min at 30 Hz using an *MM400* mixer mill (*Retsch*, Haan, Germany). An overnight extraction at 4°C was then performed using 100 mg of powdered sample, 1.0 ml of 70% methanol containing 0.1 mg/L lidocaine as an internal standard; the samples were vortexed three times during the extraction to improve the extraction efficiency. The samples were then centrifuged at 10 000 × *g* for 10 min and the supernatant was then aspirated, filtered through a microporous membrane (0.22 μm), and stored in a feed bottle for subsequent liquid chromatography-mass spectrometry analysis. The reproducibility of the samples was assessed using quality control (QC) samples that were prepared from a mixture of sample extracts and processed using the same method. During instrumental analysis, one QC sample was typically inserted for every 10 samples and analyzed to determine the reproducibility of the analytical process. The data collection instrument system mainly includes UltraPerformance Liquid Chromatography (UPLC) (*Shim-packUFLCSHIMADZUCBM20A*, http://www.shimadzu.com.cn/) and tandem mass spectrometry (MS/MS) (*Applied Biosystems4500QTRAP*, http://www.appliedbiosystems.com).

Qualitative and quantitative analysis of metabolites: After mass spectrometry analysis, the original data source was stored offline in wiff format which could be opened in the *Analyst 1.6.1* software (Zhu et al., 2013) and used for qualitative and quantitative analysis. Qualitative analysis of some substances, such as isotopic signals; repeated signals of K^+, Na^+, and NH_4^+ ions; and repeated signals of fragment ions that are themselves other substances with higher molecular mass, were removed during the analysis. Qualitative analysis of the metabolites in the samples was performed by mass spectrometry, based on the local self-built metabolite database. For metabolite structure analysis, existing mass spectrometry public databases, such as *MassBank* (http://www.massbank.jp/), *KNApSAcK* (http://kanaya.naist.jp/KNApSAcK/), *hmdb* (https://hmdb.ca/), *MoTo DB* (https://ngdc.cncb.ac.cn/databasecommons/database/id/3091), and *METLIN* (https://metlin.scripps.edu/landing_page.php?pgcontent=mainPage#), were used to integrate the peak area of the mass spectrometry peaks of all substances. The mass spectrometry peaks of the same metabolite in different samples were integrated and corrected to ensure the accuracy of quantification.

Metabolite statistical analysis: Principal component analysis (PCA) is an unsupervised multidimensional statistical analysis method that was used to reflect the overall metabolic differences between samples in each group and the magnitude of variation between samples within the group. PCA was performed on all samples using the *R package* (http://www.r-project.org/). Metabolites with variable importance in the prediction (VIP) ≥ 1 and *T*-test $P < 0.05$ were considered differential metabolites. These data were used for functional analysis of these metabolites and metabolic pathways.

Transcriptome and metabolome association analysis: To screen and obtain the collection of associated genes and metabolites that have an impact on the sample group; and analyze the association characteristics, two models were analyzed based on the two sets of data; from gene expression and metabolite abundance. The pathway functional model used inter-group difference analysis. Differentially expressed genes, obtained from the transcriptome data, and differentially expressed metabolites, obtained from the metabolome data, were used for *KEGG* enrichment analysis of the respective omics. In the association analysis, the analysis of the shared *KEGG* pathway between genes and metabolites was performed. In the correlation coefficient model, the Pearson correlation coefficient was used to measure the relationship between two variables. The strength of covariance has a range of [–1, +1]. The Pearson coefficient of gene expression and metabolite abundance was calculated to assess the correlation between genes and metabolites.

Results

Effects of GR24 on the growth of axillary buds in tobacco: The axillary bud lengths of the first to third nodes were measured 2 and 6 d after topping and showed a similar trend in all three nodes (Fig. 1*A*) with a gradual increase as treatment time increased. Two days after GR24 treatment, there was no significant difference in axillary bud length compared with the control, but the average length of the axillary buds at the three nodes was significantly lower than that of the control 6 d after treatment, indicating that the growth of axillary buds was inhibited by GR24. Thus, GR24 treatment resulted in the shortening of axillary bud length in tobacco.

RNA sequencing analysis of axillary bud response to GR24: RNA-Seq was used to analyze the gene expression profiles of tobacco axillary buds in control or after GR24 treatment. A total of 6 GB of data was obtained for each sample. After filtering the raw data, 5.14 G of clean reads were obtained with an error rate of 0.03. The Q20 percentage exceeded 97%, the Q30 percentage exceeded 93%, and the GC content exceeded 42%; indicating that the data had high accuracy and met the requirements for the bioinformatics analysis performed in this study. At least 74% of the clean reads mapped to the *Nicotiana tabacum* reference genome, of which more than 72%

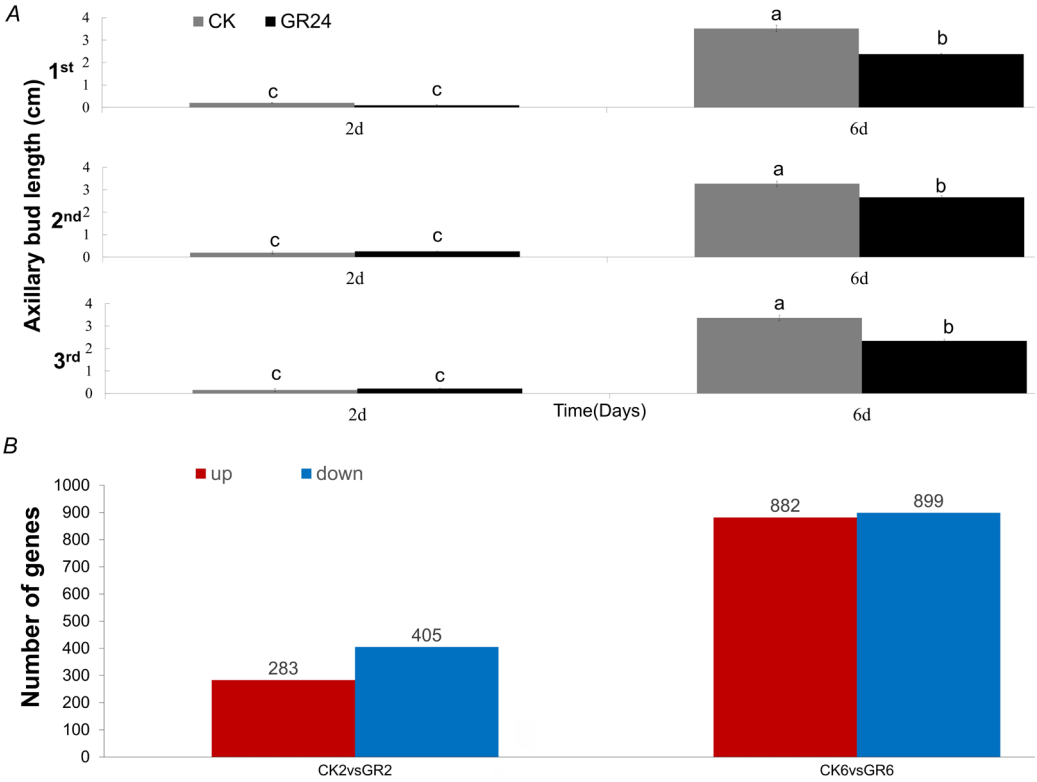

Fig. 1. Effect of strigolactone on axillary bud length in tobacco and differential gene expressions at various growth stages. *A* - The axillary bud length of the 1st to 3rd nodes at 2 and 6 d after treatment. *Different lowercase letters* indicate significant differences ($P < 0.05$). *B* - The number of DEGs in tobacco axillary buds after 2 and 6 d of treatment; CK2 (untreated axillary buds 2 d after topping), GR2 (treated axillary buds 2 d after topping), CK6 (untreated axillary buds 6 d after topping), GR6 (treated axillary buds 6 d after topping).

were uniquely mapped (Table 1 Suppl.). To validate the RNA-Seq data, we selected six DEGs for RT-qPCR analysis of GR24 treated samples. The results of RT-qPCR analysis were consistent with those for RNA-Seq, suggesting that the RNA-Seq data was accurate (Fig. 1 Suppl.).

DEGs were identified using DESeq2 (|log2fold change| ≥ 1 and FDR < 0.05). A total of 688 DEGs were identified in the CK2 *vs.* GR2 comparison group, among which 283 DEGs were upregulated and 405 DEGs were downregulated, indicating that GR24 could induce differential gene expression in the tobacco axillary bud. A total of 1 781 DEGs were identified in the CK6 *vs.* GR6 group, of which 882 DEGs were upregulated and 899 DEGs were downregulated, showing that with the extension of treatment time, GR24 has an increased effect on the expression of tobacco axillary bud genes (Fig. 1*B*).

***GO* enrichment analysis of DEGs:** In the CK2 *vs.* GR2 comparison, *GO* enrichment analysis showed that the 339 DEGs ($P < 0.05$) were enriched for 1 219 *GO* terms; of which 871 *GO* terms belonged to biological process (BP), 218 to molecular function (MF), and 130 to cellular component (CC) (Table 2 Suppl.). The top 20 significantly enriched pathways belonged to BP, and the top three enriched pathways were the cell cycle, cell cycle process, and chromatin modification (Fig. 2*A*). Therefore, after two days of GR24 treatment, the major DEGs were genes involved in biological processes related to the cell cycle; indicating that GR24 has an important effect on the cell cycle of tobacco axillary buds. In the CK6 *vs.* GR6 comparison, 915 DEGs ($P < 0.05$) were enriched for 1 625 *GO* terms; of which 1 113 belonged to BP, 359 belonged to MF, and 153 belonged to CC (Table 3 Suppl.). In BP, response to stimulus, response to stress, and response to organic substance were significantly enriched (Fig. 2*A*). For MF, the top three enriched pathways were oxidoreductase activity, oxidoreductase activity, acting on paired donors, and tetrapyrrole binding (Fig. 2*A*). For CC cell periphery and external encapsulating structure were significantly enriched (Fig. 2*A*). These results showed that in tobacco axillary buds, GR24 may be closely involved in starch and sucrose metabolism.

***KEGG* pathway mapping of DEGs:** *KEGG* enrichment analysis for DEGs from the CK2 *vs.* GR2 and CK6 *vs.* GR6 comparison groups showed enrichment in 59 and 106 *KEGG* pathways, respectively. In CK2 *vs.* GR2, the enriched pathways included protein processing in the endoplasmic reticulum (0 upregulated and 25 down-regulated DEGs), diterpenoid biosynthesis (2 upregulated and 2 downregulated DEGs), phenylpropanoid biosynthesis (5 upregulated and 6 downregulated DEGs),

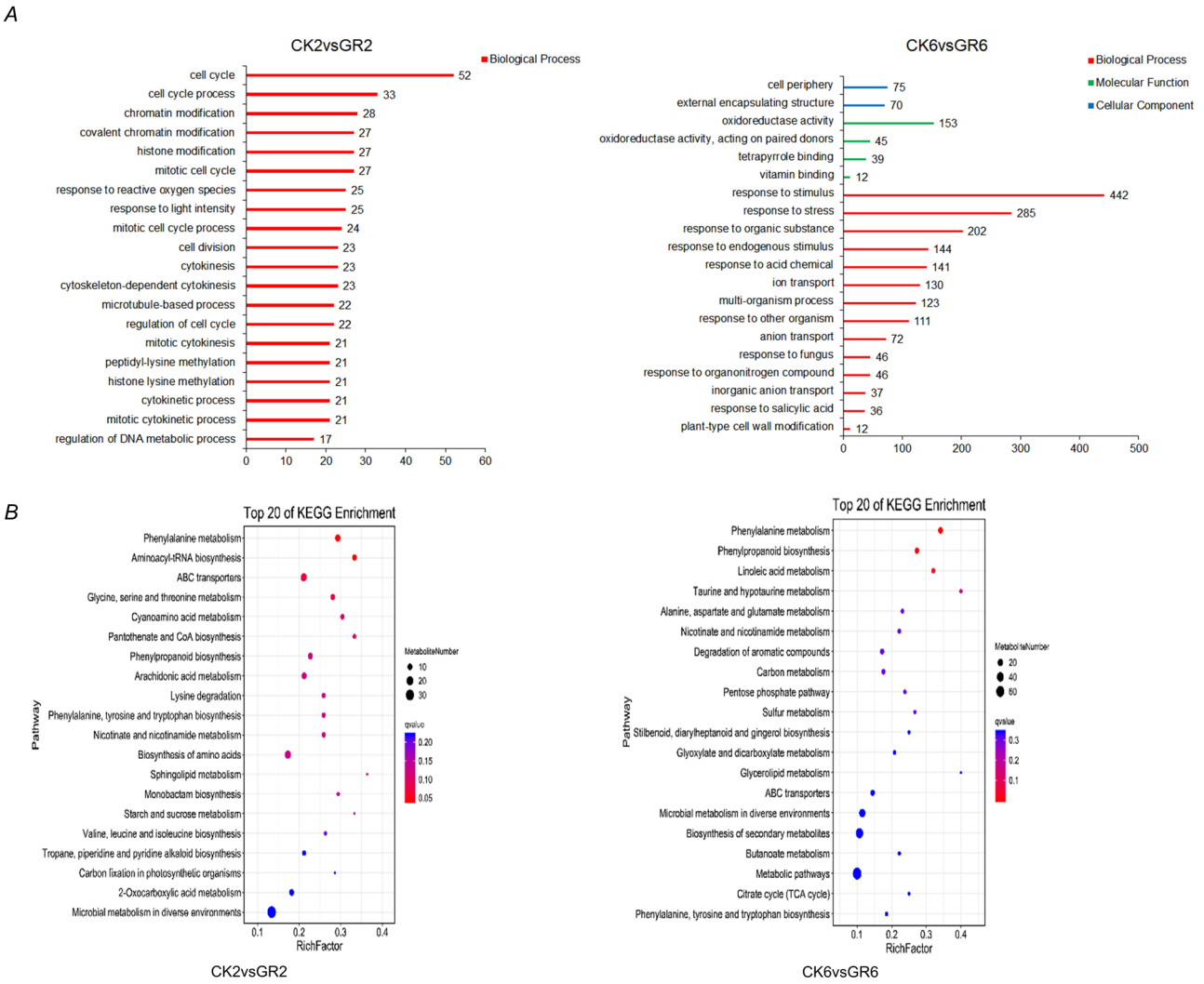

Fig. 2. *GO* and *KEGG* pathways enriched in the DEGs. *A* - Top 20 *GO* pathways enriched in the DEGs from the GR24 treatment groups compared to the control group (CK2 *vs*. GR2, *left panel*; CK6 *vs*. GR6, *right panel*). *B* - Top 20 *KEGG* pathways enriched in the DEGs from the GR24 treatment groups compared to the control group (CK2 *vs*. GR2, *left panel*; CK6 *vs*. GR6, *right panel*). Numbers beside the columns indicate the number of DEGs in that pathway. *Green*, *blue*, and *red bars* represent molecular function (MF), cellular component (CC), and biological process (BP). The size of the circles corresponds to the number of DEGs and are color-coded according to q-value. The x-axis shows the gene ratio value.

and starch and sucrose metabolism (2 upregulated and 2 downregulated DEGs) (Table 4 Suppl.). This indicates that genes related to secondary and sucrose metabolism were downregulated in response to GR24 (Fig. 2*B*). In CK6 *vs.* GR6, the enriched pathways included metabolic pathways (101 upregulated and 94 downregulated DEGs), biosynthesis of secondary metabolites (61 upregulated and 58 downregulated DEGs), metabolism of starch and sucrose (9 upregulated and 9 downregulated DEGs), and phenylpropanoid biosynthesis (22 upregulated and 5 downregulated DEGs) (Table 5 Suppl.). Compared with the CK2 *vs.* GR2 group, most secondary metabolism-related genes in CK6 *vs.* GR6 were upregulated and sugar metabolism-related genes were downregulated. This shows that GR24 treatment can affect sugar metabolism and secondary metabolite synthesis in the tobacco axillary buds.

WGCNA in axillary buds under GR24 treatment: To identify groups of genes whose expression was directly related to axillary bud length, we performed co-expression analysis and generated 17 major modules. Co-expressed genes were grouped into color-coded modules based on the similarity of their expression profiles, which were further separated by hierarchical clustering. Network heat maps of 1 000 randomly selected genes indicated a relatively high degree of independence between these clusters (Fig. 3*A*). Statistical eigengene expression was also found in the brown ($r = 0.94$, $P < 0.001$), darkmagenta ($r = 0.89$, $P < 0.001$), and saddlebrown ($r = 0.57$, $P < 0.05$) cluster genes, showing a strong positive correlation with axillary bud length (Fig. 3*B*). Genes in these modules were involved in several key pathways, including starch sucrose metabolism, phenylpropanoid biosynthesis, and secondary metabolite biosynthesis (Fig. 2 Suppl.). Therefore, GR24

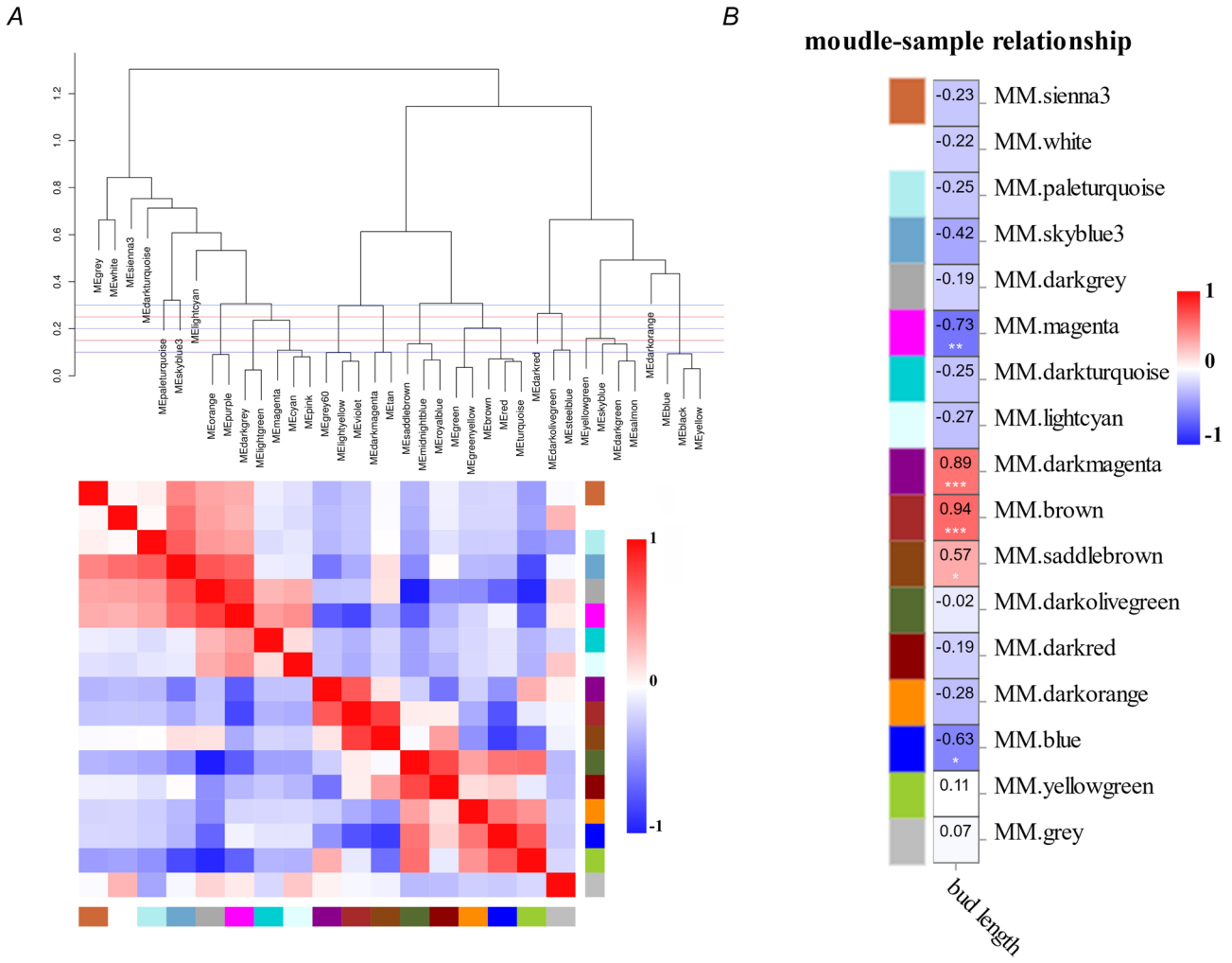

Fig. 3. WGCNA of DEGs involved in axillary bud growth. *A* - The cluster dendrogram shows 17 modules based on topologically overlapping co-expressed genes in all samples. The lower panel displays modules in specified colors. *B* - The relationship of modules to axillary bud growth. The correlation values for each module-trait pair are shown from –1 (*blue*) to 1 (*red*). The *P*-values for each module-trait comparison are shown in the graph.

may affect the growth of axillary buds by regulating starch, sucrose, and phenylpropanoid biosynthesis.

Metabolic profiling of axillary bud response to GR24: Metabolome analysis found that a total of 10425 metabolites were detected in all tobacco axillary bud samples. A total of 1 144 differential metabolites were screened using VIP ≥ 1 and *T*-test $P < 0.05$ as selection criteria. In the sample principal component analysis (PCA), the contribution of PC1 was 27.80%, and the contribution of PC2 was 20.20%. The samples in the four treatment groups were distributed in different regions and the reproducibility was good within the groups, indicating that the GR24 treatment may produce metabolic differences in the tobacco axillary buds (Fig. 4*A*). Combined with the metabolome results, the key differential metabolite changes during GR24 treatment on days 2 and 6 were analyzed. As shown in Fig. 4*B*, we identified 671 differential metabolites in CK2 *vs.* GR2 and 873 in CK6 *vs.* GR6. These are considered representative differential metabolites of the effects of GR24 treatment.

***KEGG* pathway mapping of differentially expressed metabolites:** *KEGG* enrichment analysis showed that 11 and 18 *KEGG* pathways were significantly enriched in CK2 *vs.* GR2 and CK6 *vs.* GR6, respectively ($P \leq 0.05$). In the CK2 *vs.* GR2 group, the top five enriched pathways were phenylalanine metabolism (9 upregulated and 5 downregulated DEMs); phenylpropane biosynthesis (3 upregulated and 9 downregulated DEMs); linoleic acid metabolism (8 upregulated DEMs); taurine and hypotaurine metabolism (2 upregulated and 2 downregulated DEMs); and alanine, aspartate, and glutamate metabolism (3 upregulated and 3 downregulated DEMs) (Table 6 Suppl., Fig. 4*C*). Most of these *KEGG* pathways were upregulated in axillary buds after treatment with GR24. For CK6 *vs.* GR6, the *KEGG* enriched pathways included starch and sucrose metabolism (1 upregulated and 3

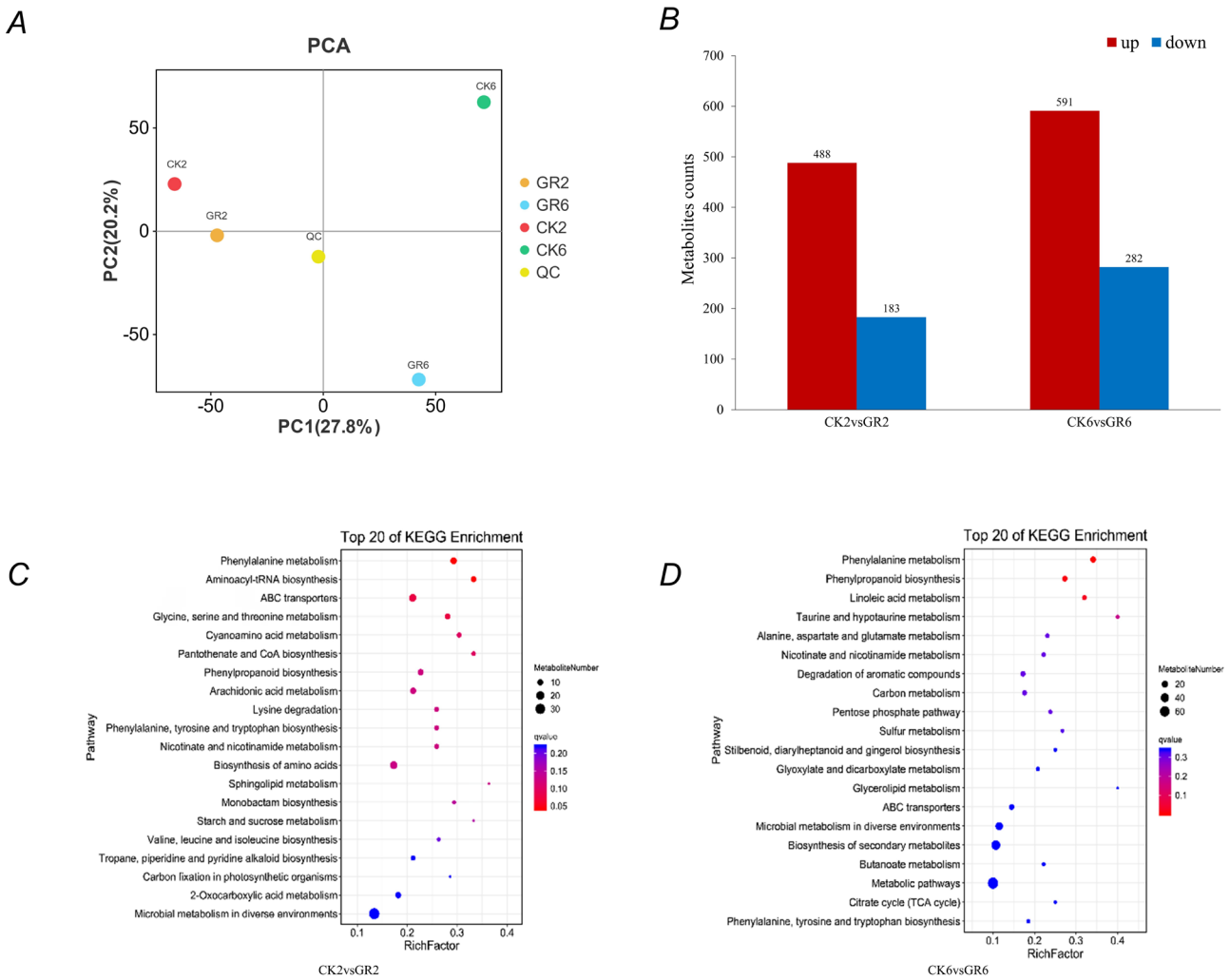

Fig. 4. Identification of accumulated metabolites after GR24 treatment in tobacco buds. *A* - PCA of five tobacco axillary bud samples and QC samples. *B* - Comparison of up and downregulated metabolites after different lengths of GR24 treatment. *C* - The top 20 *KEGG* enriched pathways for DEMs in the CK2 *vs*. GR2 treatment group. *D* -The top 20 *KEGG* enriched pathways for DEMs in the CK6 *vs*. GR6 treatment group. The size of the circle corresponds to the number of DEGs and is color coded according to the *P*-value.

downregulated), phenylalanine metabolism (3 upregulated and 9 downregulated), aminoacyl tRNA biosynthesis (3 upregulated and 6 downregulated), ATP binding cassette transporter family (7 upregulated and 9 downregulated), and glycine, serine, and threonine metabolism (1 upregulated and 8 downregulated) (Table 7 Suppl., Fig. 4*D*). Therefore, GR24 affects sugar and phenylalanine metabolism-related DEMs in tobacco axillary buds.

Conjoint analysis of DEGs and DEMs involved in key biological pathways: To further explore the effects of GR24 on genes and metabolites in tobacco axillary buds, we performed a joint transcriptomic and metabolomic analysis. In the CK2 *vs.* GR2 comparison group, the joint transcriptomic and metabolomic analysis did not identify any common enriched pathways. However, in the CK6 *vs.* GR6 comparison group, two co-enriched pathways were identified, phenylpropanoid biosynthesis and starch and sucrose metabolism (Fig. 3 Suppl., Fig. 4 Suppl.).

Expression analysis of starch and sucrose pathways in the transcriptome and metabolome: Sugar has been found to play a signaling role in the control of axillary bud growth and also promotes bud growth by inhibiting the SL signaling pathway, therefore, starch and sucrose metabolism was selected for further analysis. In the CK6 *vs.* GR6 group, starch and sucrose metabolism was enriched in 14 DEGs (five upregulated and nine downregulated) and four DEMs (one upregulated and three downregulated) (Fig. 5*A*). These DEGs were annotated and classified into eight types: sucrose synthase (SS; 2 downregulated), beta amylase (1 upregulated and 3 downregulated), and endoglucanase (1 upregulated and 2 downregulated); alpha-amylase, beta-glucosidase, and trehalose 6-phosphate phosphatase (T6P) were significantly upregulated; and sucrose-phosphate synthase (SPS) and beta-fructofuranosidase were significantly downregulated (Fig. 5*B*). The four DEMs were Robison ester, D-glucose α-1-phosphate, 1-beta-D-glucopyranosyl-

4-D-glucopyranose, and trehalose, of which only the Robison ester was downregulated DEM (Fig. 5*C*).

Correlation analysis of the starch and sucrose metabolic pathways: To understand the relationship between differential genes and differential metabolites in starch and sucrose metabolism, we created a network map based on Pearson correlation analysis. The results of the Pearson correlation analysis showed that four DEMs were strongly correlated with 12 DEGs ($P < 0.01$ and $|r > 0.900$). Only two of these DEGs, *Nitab4.5_0000157g0130* (GUS) and *Nitab4.5_0000287g0330* (AMY1), were positively correlated with Robison esters. For D-glucose alpha-1-phosphate, eight DEGs were positively correlated and two were significantly negatively correlated. For 1-beta-D-glucopyranosyl-4-D-glucopyranose, six DEGs were significantly positively correlated and two DEGs were significantly negatively correlated. For trehalose, six DEGs were positively correlated and three DEGs were significantly negatively correlated. Among these DEGs, only AMY1 was significantly correlated with four saccharide metabolism-related metabolites. *Nitab4.5_0000116g0360* (SS), *MSTRG.6436* (BMY), *Nitab4.5_0000170g0060* (SS), *Nitab4.5_0000401g0120* (SPS), and *Nitab4.5_0001383g0030* (TIV1) were positively correlated with D-glucose alpha-1-phosphate, 1-beta-D-glucopyranosyl-4-D-glucopyranose, and trehalose and could be used as candidate genes for further study of the effect of SL on axillary bud growth and development (Fig. 6).

Expression analysis of phenylpropanoid biosynthesis pathway in transcriptome and metabolome: Phenylpropanes are secondary metabolites involved in the regulation of plant growth. After 6 d of GR24 treatment, both DEMs and DEGs participating in phenylpropane biosynthesis were identified. Eighteen DEGs (15 upregulated and three downregulated) and 10 DEMs (six upregulated and four downregulated) were enriched in the phenylpropane biosynthetic transcriptome and metabolome, respectively (Fig. 7*A*). These DEGs were annotated and divided into seven types, of which all phenylpropanoid biosynthetic genes were upregulated except peroxiredoxin 6, 1-cys peroxiredoxin (*Nitab4.5_0000781g0010*), peroxidase (*Nitab4.5_0000038g0180*), and trans-cinnamate 4-monooxygenase expression (*Nitab4.5_0000404g0200*); all of which were significantly downregulated (Fig. 7*B*). In the 10 DEMs, scopoletin, trans-5-O-(4-coumaroyl)-D-quinate, 4-hydroxycinnamate, N-(3-aminopropyl)-1,4-butanediamine, trans-5-O-caffeoyl-D-quinate, and 5-hydroxyferulic acid methyl ester were upregulated (Fig. 7*C*). The results showed that these genes and metabolites may be regulated by SL to affect the growth of axillary buds.

Discussion

Tobacco is a widely cultivated crop with significant economic values and axillary bud growth is an important

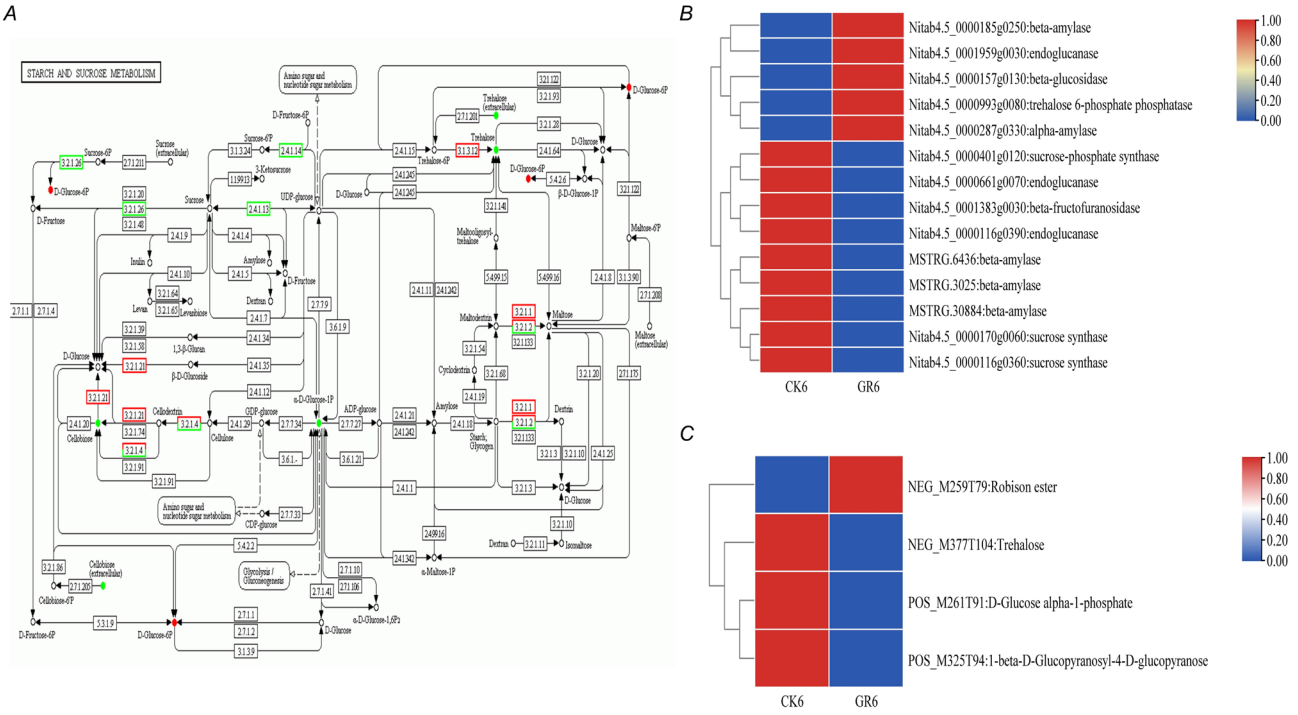

Fig. 5. The metabolic pathways of starch and sucrose, along with the expression of DEGs and DEMs, were compared between the CK6 and GR6 groups. *A* - Pathway diagram of starch and sucrose metabolism in the CK6 *vs*. GR6 comparison group. *Red squares* indicate upregulated DEGs, while *green squares* indicate downregulated DEGs. *Red dots* indicate increased DEMs, and *green dots* indicate decreased DEMs. *B* - Heat map of DEGs in starch and sucrose metabolism in the CK6 *vs*. GR6 comparison group. *C* - Heat map of DEMs in starch and sucrose metabolism in the CK6 *vs*. GR6 comparison group.

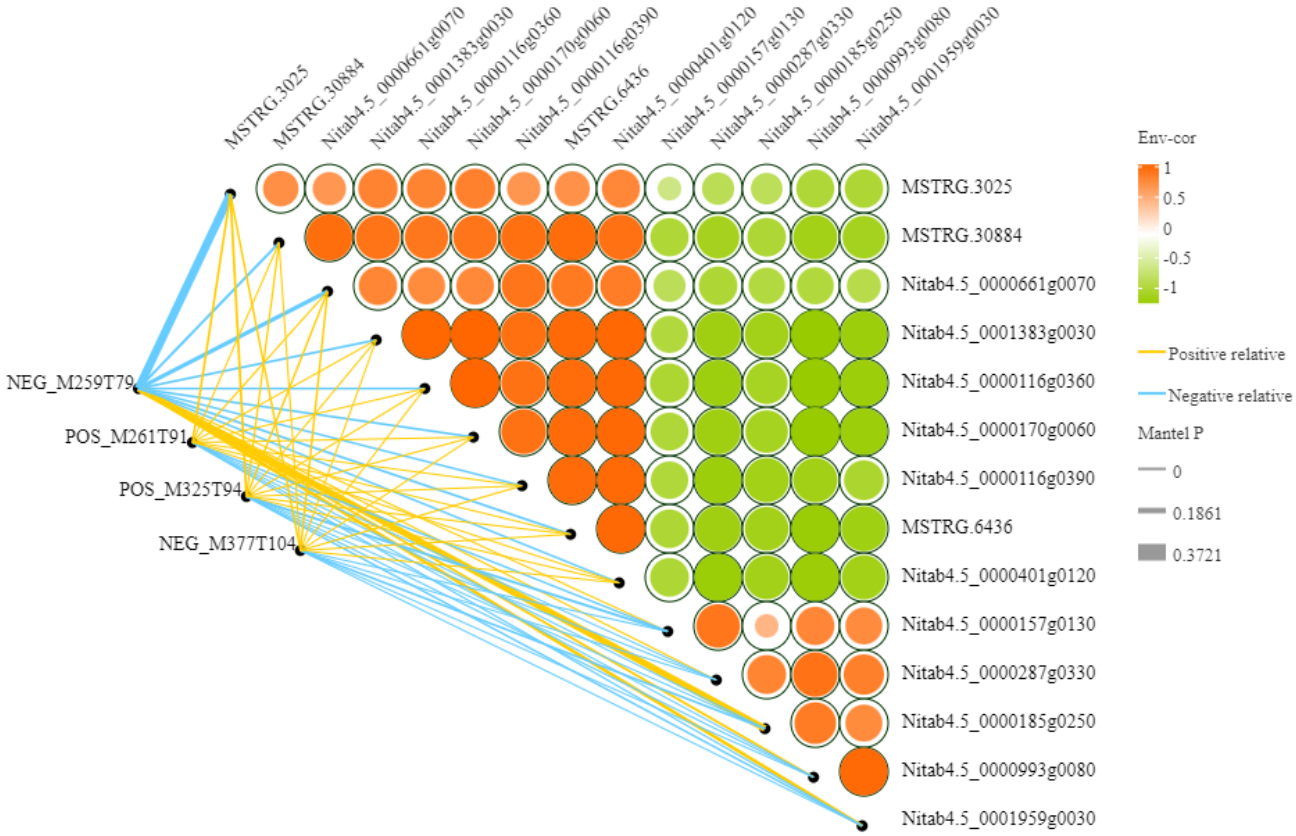

Fig. 6. Correlation analysis of the starch and sucrose metabolic pathway. *On the right side* of the heat map, the horizontal and vertical axes represent the saccharide metabolism genes associated with the GR24 response. The color of each circle in the heat map indicates the positive and negative correlation coefficients between genes, and the size of the circle indicates the absolute value of the correlation coefficients. *On the left side* of the heat map is the abundance data for metabolites in starch and sucrose metabolic pathways obtained by metabolome sequencing. These data are correlated with the data for each gene one by one by connecting lines. The thickness of the line indicates the strength of the correlation, and the color of the line indicates the significance. NEG_M259T79 – Robison ester, POS_M261T91 – trehalose, POS_M325T94 – D-glucose alpha-1-phosphate, NEG_M377T104 – 1-beta-D-glucopyranosyl-4-D-glucopyranose.

factor that affects the yield and quality of tobacco. In some studies, it has been reported that the plant hormone SL inhibits the growth of plant axillary buds (Umehara et al., 2008), therefore, it is important to understand the mechanism of this SL induced inhibition. In this study, we found that the axillary bud length of tobacco treated with GR24 was not significantly different from that of the control after two days but was significantly lower than that of the control after six days of treatment. This result may be due to insufficient treatment time. A previous study showed that GR24 had a significant inhibitory effect on the growth of non-heading Chinese cabbage axillary buds after three days and the results were consistent with those in this study (Cui et al., 2016; Dierck et al., 2016). We also compared gene and metabolite differences in axillary buds of tobacco treated with GR24 by comparative transcriptomic and metabolomic analyses and explored metabolites and potential regulatory genes involved in GR24-regulated axillary bud growth.

Transcriptome analysis can reveal a range of genes that exhibit differential expression in response to GR24 (Min et al., 2021). In this study, a total of 688 DEGs (283 upregulated and 405 downregulated) were identified in the CK2 *vs.* GR2 comparison, and a total of 1 781 DEGs (882 upregulated and 899 downregulated) were identified in the CK6 *vs.* GR6 comparison; indicating significant differences in axillary bud gene expression after GR24 treatment. *GO* enrichment analysis of the DEGs identified *GO* terms that were mainly involved in the synthesis of energy substances for both CK2 *vs.* GR2 or CK6 *vs.* GR6. *KEGG* analysis showed that starch and sucrose metabolism and phenylpropanoid biosynthesis were significantly enriched pathways in both the CK2 *vs.* GR2 and CK6 *vs.* GR6 comparisons. Therefore, GR24 treatment can regulate the metabolism of starch and sucrose to affect the growth and development of axillary buds. Previous studies have shown that sucrose can antagonize the effect of auxin by inhibiting the perception of SL, thereby promoting bud growth, and that sucrose can antagonize the inhibitory effect of SL on rice tillers. SL is also involved in the regulation of phenylpropanoid metabolism, including flavonoid synthesis and lignin deposition. These results (Dierck et al., 2016; Kotov and Kotova, 2018) are consistent with those of this study.

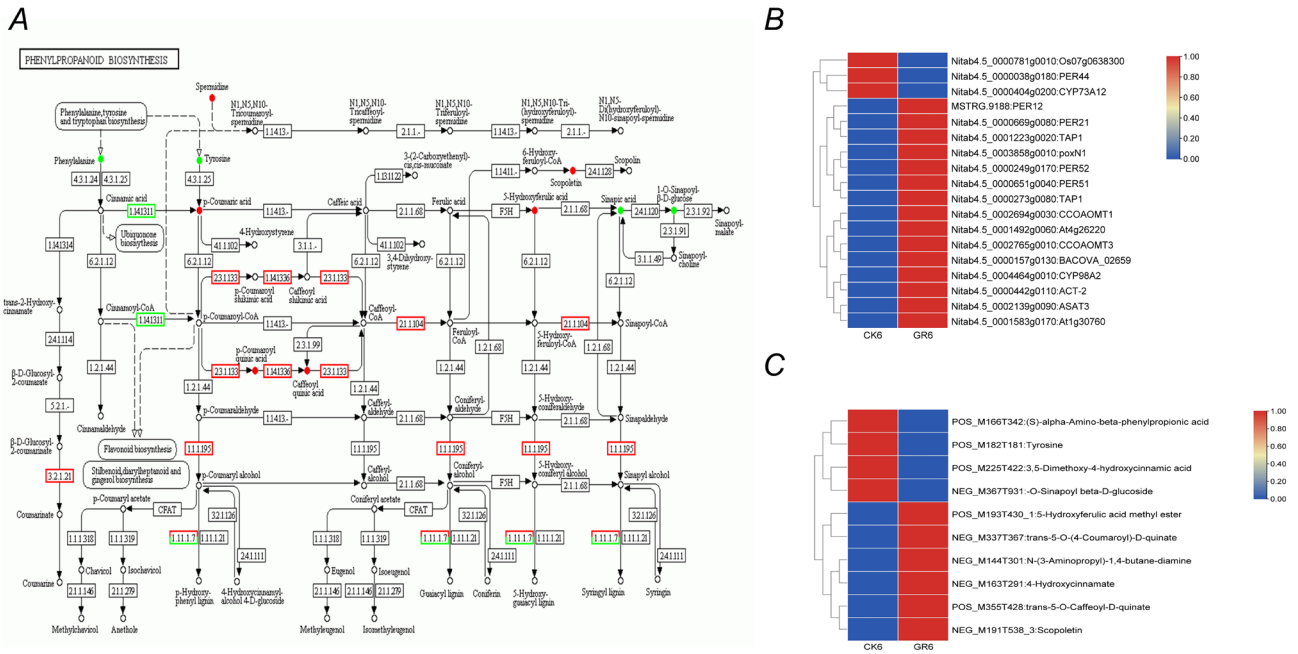

Fig. 7. The metabolic pathways of phenylpropane biosynthesis, along with the expression of DEGs and DEMs, were compared between the CK6 and GR6 groups. *A* - Pathway diagram of phenylpropane biosynthesis in the CK6 *vs*. GR6 comparison group. *Red squares* indicate upregulated DEGs, while *green squares* indicate downregulated DEGs. *Red dots* indicate increased DEMs, and *green dots* indicate decreased DEMs. *B* - Heat map of DEGs in starch and sucrose metabolism in the CK6 *vs*. GR6 comparison group. *C* - Heat map of DEMs in starch and sucrose metabolism in the CK6 *vs*. GR6 comparison group.

Sugars are important for plant growth and development, as they provide a carbon source for protein and cell wall synthesis and are an important source of energy (Stein and Granot, 2019). Recent studies have shown that sugars are important regulators of bud growth and an early signal that triggers germination activity (Mason et al., 2014). Previous studies have shown that sucrose can affect plant axillary bud development. Different types of sugars can have varying effects on axillary bud growth. Specifically, sucrose and its analogs have been found to promote axillary bud growth, while other sugars, such as glucose and fructose, may inhibit bud growth when applied exogenously. The overall effect of sugars on bud growth is thus dependent on the specific type and concentration of the sugar involved (Barbier et al., 2015b). The expression of genes related to starch and sucrose metabolism pathways stimulates the development of axillary buds in rose. SuSy (sucrose synthetase) and sucrose invertase break down sucrose into UDP-glucose and glucose, providing signaling molecules that regulate the expression of certain genes to regulate plant growth (Henry et al., 2011). The key sucrose synthase genes, *SS*, *SPS*, and *TIV1*, in this study were downregulated by SL, which is consistent with the results of previous studies. Therefore, we conclude that GR24 increases sucrose content by inhibiting the expression of starch and sucrose catabolism-related genes. *T6P* is a signaling molecule essential for plant growth and development (Yadav et al., 2014). The use of carbohydrate in *Arabidopsis thaliana* growth requires the involvement of *T6P*. There is a strong interdependence between *T6P* and sucrose content in various plant species and tissues, and low *T6P* content reflect low sucrose content (Eastmond et al., 2002; Fichtner et al., 2021). In this study, *T6P* was upregulated after GR24 treatment and the results suggest that GR24 may regulate the growth of axillary buds by increasing the sucrose content through the action of *T6P*. Robison esters are key metabolites in sugar metabolism, and their metabolic abundance is positively correlated with sucrose content. In this study, the content of Robison esters increased significantly after GR24 treatment. These results suggest that GR24 may affect the growth of axillary buds by regulating the metabolism of starch and sucrose in axillary buds.

Phenylpropanoids is a class of secondary metabolites in plants, and many studies have reported that phenylpropanoids biosynthetic pathways are closely related to plant growth and development (Deng and Lu, 2017). Phenylpropanoids metabolism is regulated by a variety of signaling pathways and regulatory mechanisms including transcriptional regulation, post-transcriptional regulation, post-translational regulation, epigenetic regulation, plant hormone signaling pathways, and biotic and abiotic stresses. Hormone regulation plays an important role in the regulation of phenylpropanoid metabolite biosynthesis. Phenylpropanoids metabolism is regulated by a variety of plant hormones such as auxin, ethylene, jasmonic acid, gibberellin, and SL. Studies have shown that SL is involved in the regulation of the phenylpropane-like metabolic pathways. Treatment with GR24 promotes the biosynthesis and accumulation of anthocyanins, whereas mutations in the SL receptor *DWARF14* gene reduce the content of anthocyanins in *Arabidopsis thaliana* (Lazar and Goodman, 2006). In *Sapium sebiferum*, overexpression of More Axillary

Branches 2 (*MAX2*), a key component encoding SL signaling, indirectly enhances anthocyanin accumulation and abiotic stress resistance (Peer et al., 2004). Studies have confirmed that phenylpropanoids inhibit the growth of axillary buds (Borevitz et al., 2000; Brown et al., 2001). Phenylalanine serves as a precursor for lignin biosynthesis in plants. Lignin is a crucial component of plant cell walls, providing structural support and participating in the regulation of plant growth and development processes. As one of the main constituents of the cell wall, lignin may affect lateral branch growth and development by influencing the mechanical properties of the cell wall and signaling pathways. The precursor compounds in the lignin metabolic pathway, such as coumarin and coumarin aldehyde, can affect the lateral growth of plants by regulating auxin synthesis and signaling. Lignin synthesis may indirectly regulate branching and growth of lateral branches by influencing the biological activity of auxin (Khadr et al., 2020). In this study, the phenylpropanoid biosynthesis pathway was upregulated by most genes and metabolites induced by GR24, suggesting that the regulation of phenylpropanoid biosynthesis pathways may be an important factor in the regulation of tobacco axillary bud growth. An in-depth study of the function of this pathway in the development of axillary buds in tobacco will provide new insights and greater understanding of the complex regulatory mechanisms of axillary bud development in tobacco.

Recent studies have extensively evaluated the molecular mechanisms through which plant hormones regulate axillary bud growth; however, the key metabolic pathways by which SL regulates axillary bud growth, especially in tobacco, are still not defined. In this study, we found that SL not only inhibited the growth of tobacco axillary buds but also had significant effects on starch and sucrose metabolism and phenylpropanoid biosynthesis pathway. Studying the key metabolic pathways during SL regulation in axillary buds can lay the groundwork for understanding the detailed mechanisms of axillary bud growth.

Conclusions

Using transcriptome and metabolome analyses, the current study revealed a complex response of tobacco axillary buds to SL. We elucidated the regulation of glucose metabolism involved in axillary bud growth in response to SL treatment and successfully identified the role of SL in key metabolite-related biological pathways in tobacco axillary buds. The study identifies a potential regulatory role of phenylpropane in the development of tobacco axillary buds, highlighting the need for further research to elucidate the underlying mechanisms. Based on transcriptomic and metabolomic data, we determined the diverse regulatory network and multiple signaling pathways involved after SL treatment. These results elucidate the comprehensive gene regulation and metabolic network involved in axillary bud growth response to SL treatment.

References

Balla, J., Medveďová, Z., Kalousek, P. et al. (2016) Auxin flow-mediated competition between axillary buds to restore apical dominance. *Scientific Reports*, 6, 35955.

Barbier, F., Péron, T., Lecerf, M. et al. (2015a) Sucrose is an early modulator of the key hormonal mechanisms controlling bud outgrowth in *Rosa hybrida*. *Journal of Experimental Botany*, 66, 2569-2582.

Barbier, F.F., Cao, D., Fichtner, F. et al. (2021) HEXOKINASE1 signalling promotes shoot branching and interacts with cytokinin and strigolactone pathways. *New Phytologist*, 231, 1088-1104.

Barbier, F.F., Lunn, J.E. & Beveridge, C.A. (2015b) Ready, steady, go! A sugar hit starts the race to shoot branching. *Current Opinion in Plant Biology*, 25, 39-45.

Bertheloot, J., Barbier, F., Boudon, F. et al. (2020) Sugar availability suppresses the auxin-induced strigolactone pathway to promote bud outgrowth. *New Phytologist*, 225, 866-879.

Borevitz, J.O., Xia, Y., Blount, J., Dixon, R.A. & Lamb, C. (2000) Activation tagging identifies a conserved MYB regulator of phenylpropanoid biosynthesis. *Plant Cell*, 12, 2383-2393.

Brewer, P.B., Dun, E.A., Ferguson, B.J., Rameau, C. & Beveridge, C.A. (2009) Strigolactone acts downstream of auxin to regulate bud outgrowth in pea and *Arabidopsis*. *Plant Physiology*, 150, 482-493.

Brown, D.E., Rashotte, A.M., Murphy, A.S. et al. (2001) Flavonoids act as negative regulators of auxin transport in vivo in *Arabidopsis*. *Plant Physiology*, 126, 524-535.

Chen, S., Zhou, Y., Chen, Y. & Gu, J. (2018) Fastp: an ultra-fast all-in-one FASTQ preprocessor. *Bioinformatics*, 34, i884-i890.

Cui, H., Cao, X., Wang, J., Xiong A., Hou, X. & Li, Y. (2016) [Effects of exogenous GR24 on the growth of axillary bud of non-heading Chinese cabbage.] *Journal of Nanjing Agricultural University*, 39, 366-372. [In Chinese]

Deng, Y. & Lu, S. (2017) Biosynthesis and regulation of phenylpropanoids in plants. *Critical Reviews in Plant Sciences*, 36, 257-290.

Dierck, R., Dhooghe, E., Van Huylenbroeck, J., De Riek, J., De Keyser, E. & Van Der Straeten, D. (2016) Response to strigolactone treatment in chrysanthemum axillary buds is influenced by auxin transport inhibition and sucrose availability. *Acta Physiologiae Plantarum*, 38, 271.

Dong, N.-Q. & Lin, H.-X. (2021) Contribution of phenylpropanoid metabolism to plant development and plant–environment interactions. *Journal of Integrative Plant Biology*, 63, 180-209.

Eastmond, P.J., Van Dijken, A.J.H., Spielman, M. et al. (2002) Trehalose-6-phosphate synthase 1, which catalyses the first step in trehalose synthesis, is essential for *Arabidopsis* embryo maturation. *The Plant Journal*, 29, 225-235.

Fichtner, F., Barbier, F.F., Annunziata, M.G. et al. (2021) Regulation of shoot branching in *Arabidopsis* by trehalose 6-phosphate. *New Phytologist*, 229, 2135-2151.

Finlayson, S.A. (2022) Branching's sweet spot: strigolactone signaling mediates sucrose effects on bud outgrowth. *New Phytologist*, 234, 7-9.

Gomez-Roldan, V., Fermas, S., Brewer, P.B. et al. (2008) Strigolactone inhibition of shoot branching. *Nature*, 455, 189-194.

Guan, J.C., Koch, K.E., Suzuki, M. et al. (2012) Diverse roles of strigolactone signaling in maize architecture and the uncoupling of a branching-specific subnetwork. *Plant Physiology*, 160, 1303-1317.

Henry, C., Rabot, A., Laloi, M. et al. (2011) Regulation of RhSUC2, a sucrose transporter, is correlated with the light control of bud burst in *Rosa* sp. *Plant, Cell and Environment*, 34, 1776-1789.
Horvath, D.P., Chao, W.S. & Anderson, J.V. (2002) Molecular analysis of signals controlling dormancy and growth in underground adventitious buds of leafy spurge. *Plant Physiology*, 128, 1439-1446.
Kaniganti, S., Bhattacharya, J., Petla, B.P. & Reddy, P.S. (2022) Strigolactone, a neglected plant hormone, with a great potential for crop improvement: Crosstalk with other plant hormones. *Environmental and Experimental Botany*, 204, 105072.
Khadr, A., Wang G.L., Wang Y.H. et al. (2020) Effects of auxin (indole-3-butyric acid) on growth characteristics, lignification, and expression profiles of genes involved in lignin biosynthesis in carrot taproot. *PeerJ*, 8, e10492.
Kim, D., Langmead, B. & Salzberg, S.L. (2015) HISAT: a fast spliced aligner with low memory requirements. *Nature Methods*, 12, 357-360.
Kotov, A.A. & Kotova, L.M. (2018) Interaction of phytohormones in regulating the axillary bud growth in pea. *Russian Journal of Plant Physiology*, 65, 628-641.
Langfelder, P. & Horvath, S. (2008) WGCNA: an R package for weighted correlation network analysis. *BMC Bioinformatics*, 9, 559.
Langmead, B. & Salzberg, S.L. (2012) Fast gapped-read alignment with Bowtie 2. *Nature Methods*, 9, 357-359.
Lazar, G. & Goodman, H.M. (2006) *MAX1*, a regulator of the flavonoid pathway, controls vegetative axillary bud outgrowth in *Arabidopsis*. *Proceedings of the National Academy of Sciences of the United States of America*, 103, 472-476.
Li, B. & Dewey, C.N. (2011) RSEM: accurate transcript quantification from RNA-Seq data with or without a reference genome. *BMC Bioinformatics*, 12, 323.
Liu, Y.-H., Yu, L., Ding, J.-H., Wuang, R.-Z., Huang, Z.-G., Xiao, L.-T. (2012) [Research progress in synergistic regulatory roles of phytohormones in shoot branching.] Plant Physiology Journal, 48, 941-948. [In Chinese]
Love, M.I., Huber, W. & Anders, S. (2014) Moderated estimation of fold change and dispersion for RNA-seq data with DESeq2. *Genome Biology*, 15, 550.
Mason, M.G., Ross, J.J., Babst, B.A., Wienclaw, B.N. & Beveridge, C.A. (2014) Sugar demand, not auxin, is the initial regulator of apical dominance. *Proceedings of the National Academy of Sciences of the United States of America*, 111, 6092-6097.
Min, Z., Li, Z., Chen, L. et al. (2021) Transcriptome analysis revealed hormone signaling response of grapevine buds to strigolactones. *Scientia Horticulturae*, 283, 109936.
Ni, J., Zhao, M.-L., Chen, M.-S., Pan, B.-Z., Tao, Y.-B. & Xu, Z.-F. (2017) Comparative transcriptome analysis of axillary buds in response to the shoot branching regulators gibberellin A3 and 6-benzyladenine in *Jatropha curcas*. *Scientific Reports*, 7, 11417.
Okazaki, K., Watanabe, S., Koike, I. et al. (2021) Strigolactone signaling inhibition increases adventitious shoot formation on internodal segments of ipecac. *Planta*, 253, 123.
Pal, N.L. & Kadam, B.S. (1949) Suppression of axillary buds in the tobacco plant. *Nature*, 164, 716-717.
Patil, S.B., Barbier, F.F., Zhao, J. et al. (2022) Sucrose promotes D53 accumulation and tillering in rice. *New Phytologist*, 234, 122-136.
Peer, W.A., Bandyopadhyay, A., Blakeslee, J.J. et al. (2004) Variation in expression and protein localization of the PIN family of auxin efflux facilitator proteins in flavonoid mutants with altered auxin transport in *Arabidopsis thaliana*. *The Plant Cell*, 16, 1898-1911.
Pertea, M., Kim, D., Pertea, G.M., Leek, J.T. & Salzberg, S.L. (2016) Transcript-level expression analysis of RNA-seq experiments with HISAT, StringTie and Ballgown. *Nature Protocols*, 9, 1650-1667.
Pertea, M., Pertea, G.M., Antonescu, C.M., Chang, T.C., Mendell, J.T. & Salzberg, S.L. (2015) StringTie enables improved reconstruction of a transcriptome from RNA-seq reads. *Nature Biotechnology*, 33, 290-295.
Qiu, Y., Guan, S.C., Wen, C., Li, P., Gao, Z. & Chen, X. (2019) Auxin and cytokinin coordinate the dormancy and outgrowth of axillary bud in strawberry runner. *BMC Plant Biology*, 19, 528.
Robinson, M.D., McCarthy, D.J. & Smyth, G.K. (2010) edgeR: a Bioconductor package for differential expression analysis of digital gene expression data. *Bioinformatics*, 26, 139-140.
Satoh-Nagasawa, N., Nagasawa, N., Malcomber, S., Sakai, H. & Jackson, D. (2006) A trehalose metabolic enzyme controls inflorescence architecture in maize. *Nature*, 441, 227-230.
Shi, J., Zhou, H., Liu, X., Wang, N., Xu, Q. & Yan, G. (2021) Correlation analysis of the transcriptome and metabolome reveals the role of the flavonoid biosynthesis pathway in regulating axillary buds in upland cotton (*Gossypium hirsutum* L.). *Planta*, 254, 7.
Stein, O. & Granot, D. (2019) An overview of sucrose synthases in plants. *Frontiers in Plant Science*, 10, 95.
Tan, M., Li, G., Chen, X. et al. (2019) Role of cytokinin, strigolactone, and auxin export on outgrowth of axillary buds in apple. *Frontiers in Plant Science*, 10, 616.
Umehara, M., Hanada, A., Yoshida, S. et al. (2008) Inhibition of shoot branching by new terpenoid plant hormones. *Nature*, 455, 195-200.
Waldie, T. & Leyser, O. (2018) Cytokinin targets auxin transport to promote shoot branching. *Plant Physiology*, 177, 803-818.
Wang, L., Wang, B., Yu, H. et al. (2020a) Transcriptional regulation of strigolactone signalling in *Arabidopsis*. *Nature*, 583, 277-281.
Wang, N., Liu, W., Yu, L. et al. (2020b) HEAT SHOCK FACTOR A8a modulates flavonoid synthesis and drought tolerance. *Plant Physiology*, 184, 1273-1290.
Yadav, U.P., Ivakov, A., Feil, R. et al. (2014) The sucrose-trehalose 6-phosphate (Tre6P) nexus: specificity and mechanisms of sucrose signalling by Tre6P. *Journal of Experimental Botany*, 65, 1051-1068.
Zhu, Z.-J., Schultz, A.W., Wang, J. et al. (2013) Liquid chromatography quadrupole time-of-flight mass spectrometry characterization of metabolites guided by the METLIN database. *Nature Protocols*, 8, 451-460.
Zwanenburg, B. & Blanco-Ania, D. (2018) Strigolactones: new plant hormones in the spotlight. *Journal of Experimental Botany*, 69, 2205-2218.